JOURNAL OF APPLIED PHYSICS 113, 153505 (2013)

Shallow-terrace-like interface in dilute-bismuth GaSb/AlGaSb single quantum wells evidenced by photoluminescence

Xiren Chen,[1] Yuxin Song,[2] Liang Zhu,[1] S. M. Wang,[2,a)] Wei Lu,[1] Shaoling Guo,[1] and Jun Shao[1,b)]

[1]*National Laboratory for Infrared Physics, Shanghai Institute of Technical Physics, Chinese Academy of Sciences, 200083 Shanghai, China*
[2]*Photonics Laboratory, Department of Microtechnology and Nanoscience, Chalmers University of Technology, SE-412 96 Göteborg, Sweden*

(Received 15 December 2012; accepted 27 March 2013; published online 15 April 2013)

Photoluminescence (PL) measurements are performed on one GaSb/AlGaSb single-quantum-well (SQW) sample and two dilute-bismuth (Bi) GaSb/AlGaSb SQW samples grown at 360 and 380 °C, at low temperatures and under magnetic fields. Bimodal PL features are identified in the dilute-Bi samples, and to be accompanied by abnormal PL blueshift in the sample grown at 360 °C. The bimodal PL features are found to be from similar origins of band-to-band transition by magneto-PL evolution. Analysis indicates that the phenomenon can be well interpreted by the joint effect of interfacial large-lateral-scale islands and Al/Ga interdiffusion due to Bi incorporation. The interdiffusion introduces about 1-monolayer shrinkage to the effective quantum-well thickness, which is similar to the interfacial islands height, and the both together result in an unusual shallow-terrace-like interface between GaSbBi and AlGaSb. A phenomenological model is established, the Bi content of isoelectronic incorporation and the exciton reduced effective mass are estimated for the GaSbBi sample grown at 380 °C, and a value of about 21 meV/% is suggested for the bandgap bowing rate of GaSbBi. An effective routine is suggested for determining the Bi content and the depth of the shallow-terraces at interface in dilute-Bi SQW structures. © *2013 AIP Publishing LLC*
[http://dx.doi.org/10.1063/1.4801530]

I. INTRODUCTION

Dilute bismuth (Bi) III–V compound semiconductors have recently attracted great attention because of the potential applications in near infrared emitters and detectors,[1] among which GaAsBi is of current interest mainly due to its large band-gap reduction,[1,2] Bi-induced temperature-insensitive emission wavelength,[3] and giant spin-orbit bowing.[4] In comparison to GaAsBi, GaSbBi is expected to manifest further advantages of efficient photoelectronic devices for the 1.55 μm optical communication window and easy realization of suppressing Auger recombination.[5] Similar to dilute nitrogen (N) compound semiconductors, the band gap of dilute-Bi semiconductor is expected to shrink relative to the non-Bi host semiconductor. However, difference is also distinct that the electronic structure effects of Bi incorporation, e.g., band anticrossing (BAC),[6] manifest mainly on valence band[7] rather than conduction band,[8] which may offer another choice for semiconductor electronic band engineering and optoelectronic applications. It is unfortunate, however, that to date experimental study of GaSbBi was very limited,[9–11] and the situation was even worse for optical investigation of low-dimensional heterostructures because of the difficulty of Bi incorporation.

Photoluminescence (PL) as nondestructive optical spectroscopy has found wide applications in characterizing electronic structures and optical properties of semiconductors,[12–15] especially for nanometer-thick thin layers of which alloy content is difficult to be determined by, e.g., x-ray diffraction (XRD) and secondary ion mass spectroscopy (SIMS). PL has been also used to study the quality and the morphology of the heterostructure interface for low dimensional semiconductor system such as quantum well or superlattice.[16–20] Interfacial atom interdiffusion and physical morphology affect the electronic structure, and lead energy shift, inhomogeneous broadening, and intensity degradation to the PL feature of band-to-band transition. Therefore, quantitative PL lineshape analysis of bandedge-related transitions can serve as an effective pathway for acquiring heterointerfacial information. Meanwhile, magneto-PL is useful for clarifying excitonic effect and possible origin of particular transitions, and has found wide applications in the low-dimensional semiconductors.[21,22] For the materials with strong bandtail states like dilute-N, however, accurate information may be drawn only when the *real* band-to-band transition is discriminated from defects-induced processes, which is unfortunately not straightforward.

In this study, PL and magneto-PL measurements are carried out at low temperatures on GaSb(Bi)/AlGaSb single quantum well (SQW) samples grown at different temperatures. Bimodal PL features are observed, and abnormal blueshift is identified for the sample grown at 360 °C while redshift is obvious for the sample grown at 380 °C. The

[a)]Electronic mail: shumin@chalmers.se
[b)]Author to whom correspondence should be addressed. Electronic mail: jshao@mail.sitp.ac.cn

 © 2013 AIP Publishing LLC

results suggest that (i) Bi-induced shallow-terrace-like interface is responsible for the bimodal PL features, which is a joint effect of Al/Ga interdiffusion and large-lateral-scale islands formation at the interface. (ii) The GaSbBi SQW sample grown at 380 °C has higher isoelectronic-incorporated Bi content, and the incorporation of Bi enhances the exciton reduced effective mass and binding energy.

II. EXPERIMENTAL DETAILS

Two $GaSb_{1-x}Bi_x$/AlGaSb and one GaSb/AlGaSb SQW samples used in this study were grown on GaSb substrate at 360, 380, and 370 °C (denoted by B360, B380, and R370 hereafter), respectively, by molecular beam epitaxy (MBE) with a structure of 5-nm-GaSb(Bi) well sandwiched by 100-nm-$Al_{0.2}Ga_{0.8}Sb$ barriers and a 10-nm-GaSb capping layer. Since Bi content of such thin SQW was difficult to be determined by XRD or SIMS, it was preliminarily assumed to be $x \simeq 0.2\%$ and 0.7%, respectively, for the B360 and B380 samples, by the XRD rocking curves and the SIMS of the GaSbBi thin films grown by the same MBE system.[5] For the speculation of possible interfacial ununiformity of the samples, 200-nm-thick GaSb(Bi) epilayers were prepared by the same MBE system at nominally identical temperatures as the samples B360, R370, and B380, respectively, and surface morphologic characterization was conducted by atomic force microscopic (AFM) technique.[5]

PL measurements were conducted with a spectral resolution of 1 meV (or equivalently, 8 cm^{-1}) using a Fourier transform infrared (FTIR) spectrometer (Bruker IFS 66v/S) in the rapid- rather than step-scan mode.[13,22] Ar^+ laser at 514.5-nm line was used together with a laser power controller to warrant a stable excitation at 60 mW. The luminescence signal was detected by a room temperature InGaAs detector. The samples were cooled down either by liquid nitrogen to about 77 K or by continuous flow liquid helium to about 3.8 K. Detailed description of the PL system and experimental configuration can be found elsewhere.[13,20] Magnetic fields of up to 10 T were built up using a superconducting optical magnet in Faraday configuration.[21,22] The spatial distance between the FTIR spectrometer and the optical magnet was far enough to guarantee the elimination of the interference on the instrument performance by magnetic field.

III. RESULTS AND DISCUSSION

Figure 1(a) illustrates a PL spectrum and its inverted second-order derivative (SOD) of the R370 GaSb/AlGaSb SQW sample at 77 K.

The slightly asymmetric single-peak SOD lineshape hints a dominant PL process accompanied by a close-positioned high-energy weak PL process, and the peak corresponds to the energy of the dominant PL process. The transition energy of the dominant PL process is determined[22] as 0.9229 eV. To account for the asymmetry of the PL lineshape, gravity-center (GC) energy is also estimated as 0.9249 eV by taking the total PL transitions as a single visual process, the position is marked by the vertical bar in Fig. 1(a). Similarly, the dominant PL and the GC energies are determined as 0.9310 and 0.9288 eV for the B360, and 0.9194 and 0.9172 eV for the B380 GaSbBi/AlGaSb SQW samples at 77 K, the results are indicated by the vertical arrows and bars in Fig. 1(b) together with that of the R370 GaSb sample. The difference of the dominant PL and GC energies is plotted as inset in Fig. 1(b) for all the three samples. The dots represent the peak energies, while the open triangles the GC energies.

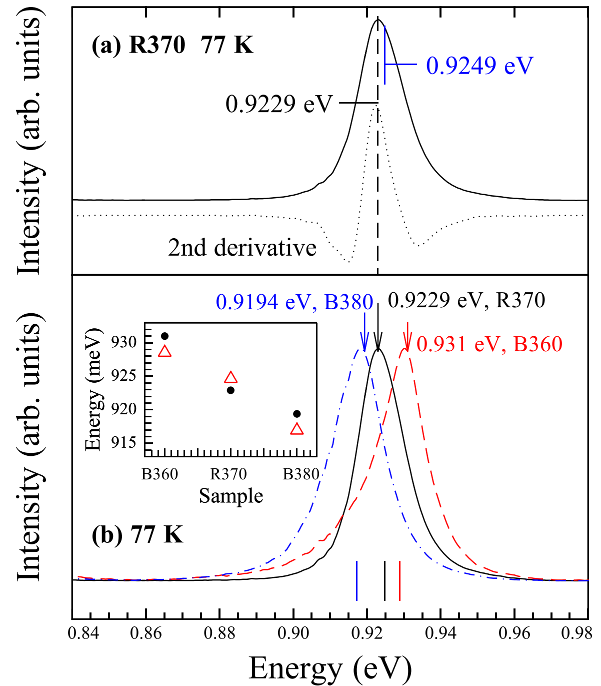

FIG. 1. (a) PL spectrum and its inverted second derivative of R370 GaSb/AlGaSb SQW sample at 77 K, vertical dashes for peak position and vertical bar for GC energy. (b) Normalized PL spectra of B360 and B380 GaSbBi/AlGaSb and R370 GaSb/AlGaSb SQW samples. Peak energies by vertical arrows and digits, and GC energies by bars at the bottom. Inset shows peak and corresponding GC energies (dots and open triangles).

The PL spectra of the two dilute-Bi samples manifest typical features as widely observed in dilute-N materials,[23,24] i.e., one dominant PL process of band-to-band transition and a close-positioned weak bandtail of defect-/interfacial roughness-related localization. The PL peak of B380 redshifts relative to R370, due to the Bi isoelectronic incorporation-induced valence-band shifting and bandgap shrinking as predicted by the BAC theory. It is strange, however, that B360 manifests an abnormal blueshift of the PL peak relative to R370, which is difficult to understand solely with the BAC model.

As the linewidth of PL feature is determined by homogeneous and inhomogeneous broadening, of which the former gets enhanced at higher temperatures when phonon scattering comes into force,[25] similar PL measurements are performed at a low temperature of 3.8 K to diminish the homogeneous broadening. The results are shown in Fig. 2. The peak energy is again determined by the SOD as 0.9307 eV for R370. For the GaSbBi samples, however, two features are identified with energies of 0.9309 and 0.9385 eV for B360, and 0.9202 and 0.9263 eV for B380. The GC energies are also estimated as 0.9288, 0.9305, and 0.9214 eV, respectively, for the samples R370, B360, and B380. The difference of the dominant PL and GC energies is plotted as inset in Fig. 2 for all the

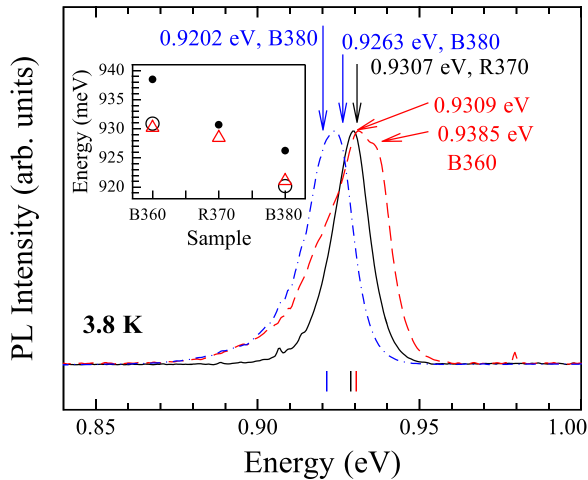

FIG. 2. Normalized PL spectra of the samples R370, B360, and B380 at 3.8 K. 2nd-derivative energies marked by arrows and digits, and GC energies by vertical bars. Inset: 2nd-derivative energies as dots and open circles, and GC energies as open triangles, respectively.

three samples. The dots and open circles represent the SOD energies, and the open triangles show the GC energies.

The PL spectrum of R370 manifests a similar lineshape as that at 77 K, and the difference of the GC energies between 3.8 and 77 K is 3.9 meV. For the GaSbBi samples, however, bimodal rather than unimodal features are identifiable with an energetic separation of 7.6 meV for B360 and 6.1 meV for B380. The difference of the GC energies between 3.8 and 77 K is 4.2 meV for B380, close to that of R370, but 1.7 meV for B360, which is much smaller than that of the other two samples. The energy of the lower-energy PL feature of B360 (as indicated by open circle in the inset of Fig. 2) is nearly identical to the energy of the dominant peak of R370 (as indicated by dot in the inset). The abnormal blueshift of B360 at 77 K seems to be the effect of carrier population in a higher-energy state, of which the transition energy is 0.9385 eV at 3.8 K and the origin will be clarified later when a phenomenological model is devised for Bi effect. Homogeneous broadening merges the PL features to a broader peak, while the difference of GC energy between 3.8 and 77 K is a hint for carrier population in higher-energy state.

To clarify the mechanisms of the PL features and to verify if they reflect excitonic effects, magneto-PL measurements are conducted at 3.8 K under Faraday configuration[21,22] at various magnetic fields up to 10 T. Representative spectra are depicted in Fig. 3. Curve fittings with a mixture of Lorentzian and Gaussian (MLG) functions are performed,[20,25] the results are plotted also in Fig. 3 as dots, dashes, and dashed-dots, respectively.

The PL spectra of R370 are as illustrated in Fig. 3(a) well reproduced by a dominant feature (denoted by DF) centered at 0.9302 eV at 0 T and a defects and/or interfacial roughness-induced localized states-related bandtail, which is of typical PL characteristic of QW structures.[25] The former should originate from the band-to-band transition. It is worthy to mention that the DF energy at 0 T is nearly identical to that derived by the SOD, indicating the reliability of the MLG fittings. For B360 and B380, on the other hand, four MLGs are needed in reproducing the magneto-PL spectra as illustrated in Figs. 3(b) and 3(c), of which the two PL features at high energy side correspond to the bimodal features identified in Fig. 2 and are denoted by low-energy feature (LEF) and high-energy feature (HEF), the third is broad and strong feature denoted by BSF, and the fourth with the lowest energy is of bandtail characteristic just as that of R370. The energies of LEF and HEF are 0.9312 and 0.9381 eV for B360, and 0.9205 and 0.9266 eV for B380 at 0 T. The ratio of the LEF and HEF integral intensities is about 33.2% and 48.3%, respectively, for B360 and B380, indicating the population of the higher-energy state to be relatively higher for B360. This is in good agreement with the above judgment from the difference of the GC energies at 3.8 and 77 K.

For the BSF in the samples B360 and B380, correlation to inhomogeneous broadening can be assumed based on the facts that: (i) the BSF only shows up in the GaSbBi samples, (ii) its energy is lower than that of the LEF and HEF, and (iii) it is only of Gaussian lineshape in the whole magnetic fields of 0–10 T. As Bi is known to create bound states and disorder of the structure matrix,[2,26] the BSF can thus be assigned to the structure disorder-related transitions in the GaSbBi samples. For the LEF and HEF, the mechanism seems to be unlikely the inhomogeneous Bi incorporation simply due to the PL blueshift of B360 relative to R370. In contrast, these features may directly correlate to the band-to-band transitions in different parts of the QW layer with considerable difference in thickness introduced by interfacial large-lateral-scale islands. Recent AFM experiment indicated that the incorporation of Bi in GaSb thin film may result in regular step-like terraces or islands at the surface with a lateral scale of $\sim 10^2$ nm and thickness of $\sim 10^{-1} - 10^0$ nm, which is more significant than the GaSb reference sample.[5] Meanwhile, a thickness difference of 1 monolayer (ML, or about 0.3 nm) in 5-nm-thick $GaSb/Al_{0.2}Ga_{0.8}Sb$ SQW will lead to about 6 meV change to the band-to-band transition energy, according to the effective-mass approach for finite-depth QW[27] with an 80-meV valence-band offset[28] and without nonparabolic effects. As the excitation laser spot is at a size of 10^2 μm and especially, the energy difference between LEF and HEF is about 7 meV for B360 and 6 meV for B380, the bimodal PL features of LEF and HEF are likely a sign of the formation of

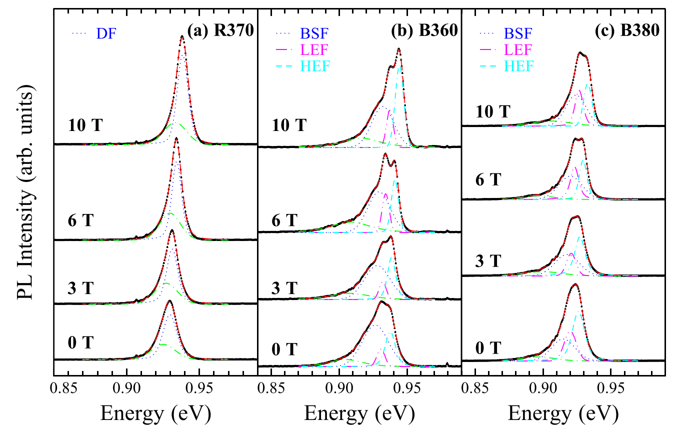

FIG. 3. Representative magneto-PL spectra and curve fittings of R370 (a) GaSb/AlGaSb, and B360 (b) and B380 (c) GaSbBi/AlGaSb SQW samples at 3.8 K. Dots in (a) for DF of R370. Dots, dashed-dots, and dashes in (b) and (c) for the curve fittings of BSF, LEF, and HEF of B360 and B380, respectively.

terraces or islands across the interface between the GaSbBi well and the AlGaSb barrier layers.[5]

It is worthy to mention that bimodal PL features were also observed in GaAs/AlAs quantum wells.[16,18] However, there is a significant difference between the bimodal PL of GaAs/AlAs QWs[16,18] and that of GaSbBi SQW in this study. The interfacial islands result in PL redshift for the GaAs/AlAs QWs because of the low-energy-state occupation of carriers at low temperature, while abnormal blueshift in B360 GaSbBi SQW sample is observed in this study, indicating different mechanism for the bimodal PL in GaAs/AlAs and GaSbBi QW systems.

Figure 4 plots the energies of the DF, LEF, and HEF, respectively, as squares, open stars, and dots, against magnetic field for the three samples. The LEF and HEF of B360 are upshifted by 5 meV for clarity. Clearly, all the features manifest typical diamagnetic shift, indicating the nature of excitonic transition.[21] The BSF and the bandtail feature in Fig. 3, on the other hand, cannot be assumed with diamagnetic shift because of strong fluctuation of the energies around a baseline.

The evolutions of the features' energies with magnetic field are fitted as solid lines by a quasi-two-dimensional exciton effective-mass equation[21,22]

$$\left\{-\frac{\hbar^2}{2\mu}\left[\frac{1}{\rho}\frac{\partial}{\partial\rho}\left(\rho\frac{\partial}{\partial\rho}\right)\right]+\frac{e^2}{8\mu}B^2\rho^2-V(\rho)\right\}R_n(\rho)=E_nR_n(\rho),$$
$$V(\rho)=\frac{e^2}{4\pi\varepsilon_0}\int_{-\infty}^{+\infty}\frac{|Z_e(z_e)|^2|Z_h(z_h)|^2}{\varepsilon_r(z_e,z_h)\sqrt{\rho^2+(z_e-z_h)^2}}dz_edz_h, \quad (1)$$

where μ is the exciton reduced effective mass. ρ is the extent of the excitonic in-well-plane wave function. $Z_e(z_e)$ and $Z_h(z_h)$ are the wave functions of electrons and holes in confined direction, respectively. ϵ_0 and ϵ_r are the absolute and relative permittivity of the material, respectively. The subscript n represents the nth excitonic state. $R_n(\rho)$ is the envelope function of S symmetry exciton. The results are depicted as lines in Fig. 4. With this procedure, the exciton reduced effective mass and binding energy are derived for the DF of the sample R370, LEF and HEF of the samples B360 and B380, and are listed in Table I in the unit of m_0 and meV, respectively.

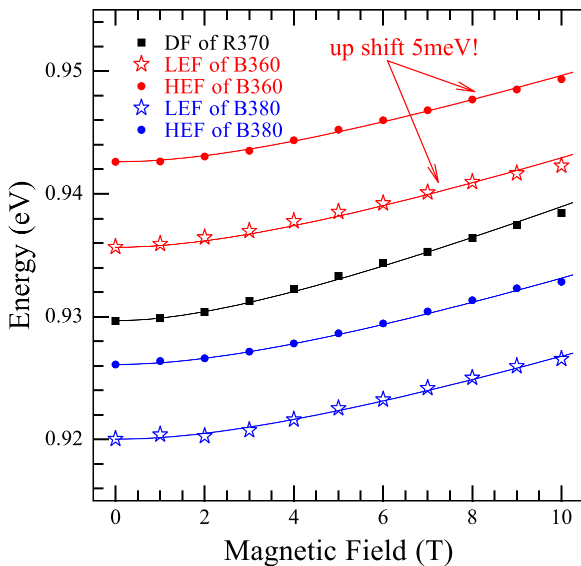

FIG. 4. PL energies of DF of R370 GaSb/AlGaSb, and LEF and HEF of B360 and B380 GaSbBi/AlGaSb SQW samples at 3.8 K, respectively, as a function of magnetic field. Solid lines are the fittings with an exciton effective-mass approach. LEF and HEF of B360 are up-shifted by 5 meV for clarification.

TABLE I. Exciton reduced effective mass (μ, in the unit of m_0) and binding energy (E_b, in the unit of meV) of the DF of GaSb/AlGaSb SQW sample R370, and the LEF and HEF of GaSbBi/AlGaSb SQW samples B360 and B380.

	B360		R370	B380	
	LEF	HEF	DF	LEF	HEF
μ	0.0365	0.0373	0.0315	0.0382	0.0373
E_b	7.67	7.79	6.88	7.93	7.79

It is obvious that the excitonic effects in the dilute-Bi samples B360 and B380 are enhanced relative to the R370 reference sample, while the difference between the two dilute-Bi samples is relatively small. In addition, the effects are similar for the LEF and HEF, with less than 2.5% difference in either reduced effective mass or exciton binding energy, and the exciton radii of the LEF and HEF are both about 20 nm, much smaller than the lateral scale of the terraces revealed by the AFM morphology of GaSbBi thin film.[5] Figure 5 shows the AFM surface morphology of an area of $3\times3\,\mu m^2$ of 200-nm-thick GaSb(Bi) thin film with the growth condition as B360 (a), R370 (b), and B380 (c). It is seen in Figs. 5(a) and 5(c) that obvious large-lateral-scale islands emerge only in the dilute-Bi films. The lateral scale of the islands is estimated to be at a level of 10^2 nm, by which a similar size of islands can be projected to the SQW structure if the in-plane strain in the 5-nm-thick QW layer is taken as the same as the 200-nm-thick thin film. It was shown that the lateral scale of the island is mainly determined by the crystal strain,[29] within the critical thickness of the thin layer. The root mean square (RMS) is about 0.294 nm, 0.185 nm, and 0.298 nm, respectively, for the three samples, indicating significantly rougher surface for the GaSbBi thin films. These results suggest the mechanism of the LEF and HEF processes as band-to-band transitions with different QW thicknesses. Such a difference in QW thickness is, however, different from the case as GaAs/AlAs QW[16,18] with quantum islands at the interface, because of the abnormal blueshift in the GaSbBi sample B360 as mentioned above.

To well understand the experimental observation, a phenomenological model is proposed as illustrated in Fig. 6, based on the interfacial larger-lateral-scale islands and the atomic interdiffusion at the interface. Bi was recently indicated as a potential factor for increasing the III-group atomic interdiffusion in alloys.[30] Thus, Al/Ga interdiffusion across the GaSbBi/AlGaSb interface is enhanced. The energy difference between the LEF and HEF is about 7 meV for B360, which corresponds to about 1.1-ML-thick interfacial islands induced by Bi incorporation as schematically illustrated in Fig. 6(a). On the other hand, as the LEF energy of B360 is almost equal to, and the HEF energy takes a blueshift

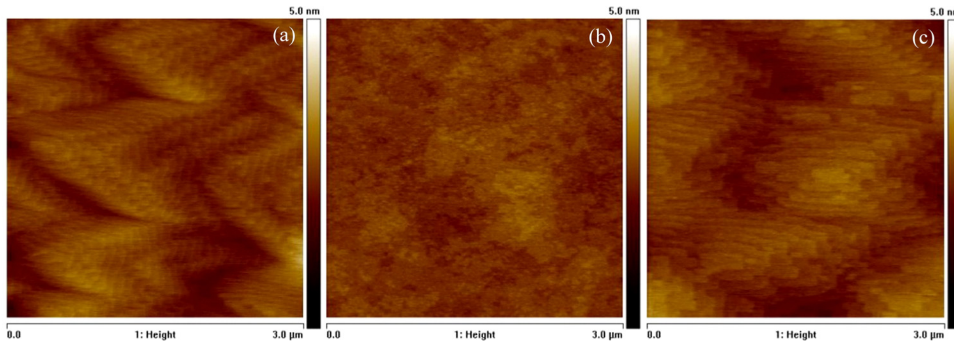

FIG. 5. AFM surface morphology of an area of $3 \times 3\,\mu m^2$ of 200-nm-thick GaSb(Bi) thin film with the growth condition as B360 (a), R370 (b), and B380 (c), respectively, with a root mean square of about 0.294 nm, 0.185 nm, and 0.298 nm.

relative to the DF energy of R370, the isoelectronic Bi content in B360 can be negligible, and the Al/Ga interdiffusion is equivalent to a shrinkage of QW thickness by 1.2 ML according to the blueshift of HEF, as indicated in Fig. 6(b). The interdiffusion-induced shrinkage of QW thickness neutralizes the effect of the islands, and results in shallow terraces where there are initially not islands. The joint effect of the islands and the Al/Ga interdiffusion at the interface both induced by Bi incorporation is as a consequence the emergence of an effective shallow-terrace-like interface structure at the GaSbBi QW side as shown in Fig. 6(c). The LEF should hence correlate to the band-to-band transition of 5-nm-thick QW, while the HEF the band-to-band transition of the shallow-terrace related part of the QW, respectively. Large amount of the shallow terraces and significant thermalization of the carriers initially distributed in the LEF related states lead to a blueshift of the PL peak for the GaSbBi sample B360 at 77 K as aforementioned.

It is interesting to note that the formation of the interfacial large-lateral-scale islands in GaSbBi thin films is also justified by the difference in the AFM surface morphology from the GaSb thin film as illustrated in Fig. 5. While the both GaSbBi thin films grown at 360 and 380 °C show clear lateral-scale islands with a RMS of about 0.30 nm, the GaSb thin film grown at 370 °C does not show such lateral-scale islands obviously, and the RMS of the surface morphology is only about 0.19 nm.

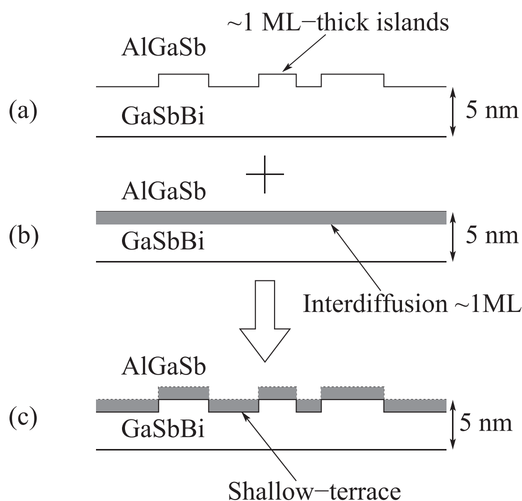

FIG. 6. Schematic for the formation of shallow-terrace-like interface (c) in B360 and B380 GaSbBi/AlGaSb SQW samples due to Bi-enhanced interfacial large-lateral-scale islands (a) and atomic interdiffusion (b).

Taking into account the facts that (i) the LEF of B360 shows up at nearly the identical energetic position as, while the LEF and HEF of B380 redshift relative to the DF of R370, and (ii) the BSF correlating to structural disorder is more significant for B360, preliminary conclusion can be drawn that lower growth temperature generates more disorder and defects, and the Bi-induced bandgap reduction should be very small. At a higher growth temperature of 380 °C, Bi tends to occupy the substitutional sites to shrink the bandgap energy by rising the topmost valence band, and the effect of the shallow-terraces is surpassed, which leads to about 10 meV redshift at 3.8 K. The large difference in PL intensities of the dominant band-to-band and bandtail transitions in the GaSb sample R370, on the other hand, suggests a superior interface and structure quality over the dilute-Bi counterparts.

The exciton reduced effective mass and binding energy of the LEF of B380 are about 21% and 16% larger than those of the DF of R370, respectively. This is in agreement with the established knowledge that dilute-Bi isoelectronic incorporation enlarges the reduced effective mass.[31] For B360, the Bi isoelectronic incorporation should be very limited, the enlarged reduced effective mass should therefore not mainly be the isovalent Bi effect. Previous $\mathbf{k}\cdot\mathbf{p}$ simulation indicated that structural disorder may result in an increase to the effective mass.[32] As the BSF features are also related to the structural disorder and the proportions in integral intensity are about 55% and 29%, respectively, for B360 and B380 at 0 T, the effective mass enlargement may be correlated to structural disorder in the GaSbBi sample B360 while it should be a joint effect of disorder and Bi isoelectronic incorporation in the GaSbBi sample B380.

The combination of the temperature and magnetic-field effects on PL properties leads to a qualitative description of Bi in dilute-Bi GaSb QW layer that Bi atoms exert mainly two influences on GaSb/AlGaSb SQW of (i) incorporating into the substitutional sites to form a *real* dilute-Bi ternary compound, and (ii) resulting in the formation of shallow-terraces-like interface structure. While the former results in a bandgap reduction and exciton enhancement as clearly seen in the GaSbBi SQW sample B380, the latter forms a partial narrower QW which corresponds to higher transition energy and disorder-enhanced two-dimensional excitonic effects as evidenced in the GaSbBi SQW sample B360. Growth temperature dominates Bi behavior. At a growth temperature of 380 °C, Bi atoms are encouraged to occupy substitutional sites, the bandgap shrinkage surpasses the shallow-terrace

interface effect. At 360 °C, however, low-terrace effect dominates and leads to an overall PL blueshift.

Implications are as follows noteworthy for the identification of Bi effects in QWs: (i) The LEF at extremely low temperature is considered as the *real* band-to-band transition with the nominal QW thickness, its redshift relative to the DF of the reference GaSb sample can be used for bandgap bowing[1] analysis reliably. (ii) The energy separation as well as the relative strength of the LEF and HEF can serve as a judgment for the degree of the low-terraces depth and the distribution of the unidirectional terraces. (iii) The LEF of the sample B380 redshifts by 9.7 meV relative to the reference sample R370. It corresponds to about 15 meV up-shifting of the topmost valence-band edge, with the assumption that Bi isoelectronic doping only rises the topmost valence band within the approach of model-solid theory[27]

$$\Delta E_{\text{offset}} = E_{\text{con}} \left[\frac{m_w^*}{m_w^* + m_b^* \tan^2(kL/2)} \right]^{-1/2}, \qquad (2)$$

where ΔE_{offset} is the valence-band offset between the QW and the barrier layers, E_{con} is the confinement energy of the first confined hole level, m_w^* and m_b^* are the carrier effective masses in the QW and the barrier layers, respectively, L is the QW width, k is the wave vector given by $k = \sqrt{2m_w^* E_{\text{con}}}/\hbar$. The bandgap bowing rate of GaSbBi is hence estimated to be about 21 meV/% if the Bi content is taken as 0.7% as that of thin film.

It is worthy to mention that two significantly different values of 33 meV/%[9] and 100 meV/%[11] were previously suggested. However, if the facts are taken into account that (i) in the BAC theory, the bandgap bowing in dilute-Bi material is due to the interaction of the resonant Bi energy level with the topmost valence-band edge of the host material, (ii) the absolute Bi energy level does not vary significantly in different matrix,[7] and (iii) the topmost valence-band edge of GaSb is higher than that of GaAs,[33] it is rather safe to consider that the bowing rate of GaSbBi should not be lager than that of GaAsBi, i.e., 88 meV/%.[1] On the other hand, if the bandgap bowing rate is taken as 33 meV/% as bulk structure,[9] the Bi content should be about 0.45%, which is obviously lower than that derived by XRD and SIMS in the thin film,[5] and hence a higher Bi exhalation has to be assumed for low dimensional structure during MBE growth process. In contrast, it seems to be very reasonable to take the value of 21 meV/% for the bandgap bowing of GaSbBi, because the topmost valence-band edge position of InSb is close to that of GaSb[33] and a bowing rate of about 19 meV/% was suggested for InSbBi.[34] From this aspect, this study not only reveals the shallow-terrace-like interface structure but may also serve as an effective routine for characterizing Bi content and/or bandgap bowing effect of dilute-Bi QWs.

IV. SUMMARY

To summarize, PL and magneto-PL measurements were conducted on two GaSbBi/AlGaSb SQW samples grown at 360 and 380 °C, and one GaSb/AlGaSb SQW sample grown at 370 °C as reference. While redshift as foreseen by the BAC model was clearly seen in the sample grown at 380 °C, an abnormal blueshift was observed in the sample grown at 360 °C. Bimodal PL features with the similar transition origins were identified for both the GaSbBi samples by diamagnetic shift behavior. The experimental results indicate the existence of an interfacial effective terrace-like structure in the GaSbBi/AlGaSb SQW which is unidirectional to shrink the quantum well thickness other than the interfacial islands or regular bidirectional interfacial roughness. A phenomenological model is proposed to well understand the emergence of this interfacial structure based on the large-lateral-scale interface islands and the interfacial Al/Ga interdiffusion both enhanced by Bi incorporation. Analysis suggests that Bi atoms tend to occupy the substitutional position at growth temperature of 380 °C, and Bi isoelectronic incorporation enhances the excitonic reduced effective mass and binding energy. A value of about 21 meV/% is derived for the bandgap bowing of GaSbBi. The movement of PL peak and the energy difference of bimodal features may serve as a measure for the Bi content and the depth of shallow terraces at interface.

ACKNOWLEDGMENTS

One of the authors (C.X.R.) thanks Xiang Lü for helpful discussion. The work was sponsored by the SITP KIP (QZY74), the STCSM (11JC1413800), and the NSFC (11274329 and 61176075) of China.

[1]S. Francoeur, M. Seong, A. Mascarenhas, S. Tixier, M. Adamcyk, and T. Tiedje, Appl. Phys. Lett. **82**, 3874 (2003).
[2]S. Francoeur, S. Tixier, E. Young, T. Tiedje, and A. Mascarenhas, Phys. Rev. B **77**, 085209 (2008).
[3]J. Yoshida, T. Kita, O. Wada, and K. Oe, Jpn. J. Appl. Phys., Part 1 **42**, 371 (2003).
[4]B. Fluegel, S. Francoeur, A. Mascarenhas, S. Tixier, E. Young, and T. Tiedje, Phys. Rev. Lett. **97**, 67205 (2006).
[5]Y. Song, S. Wang, I. Saha Roy, P. Shi, and A. Hallen, J. Vac. Sci. Technol. B **30**, 02B114 (2012).
[6]W. Shan, W. Walukiewicz, J. W. Ager, E. E. Haller, J. F. Geisz, D. J. Friedman, J. M. Olson, and S. R. Kurtz, Phys. Rev. Lett. **82**, 1221 (1999).
[7]K. Alberi, J. Wu, W. Walukiewicz, K. Yu, O. Dubon, S. Watkins, C. Wang, X. Liu, Y. Cho, and J. Furdyna, Phys. Rev. B **75**, 045203 (2007).
[8]J. Shao, W. Lu, M. Sadeghi, X. Lü, S. Wang, L. Ma, and A. Larsson, Appl. Phys. Lett. **93**, 031904 (2008).
[9]V. Germogenov, Y. Otman, V. Chaldyshev, and Y. Shartsev, Sov. Phys. Semicond.-USSR **23**, 942 (1989).
[10]P. Gladkov, E. Monova, and J. Weber, J. Cryst. Growth **146**, 319 (1995).
[11]S. Das, T. Das, S. Dhar, M. de La Mare, and A. Krier, Infrared Phys. Technol. **55**, 156 (2012).
[12]A. Mascarenhas, S. Kurtz, A. Kibbler, and J. Olson, Phys. Rev. Lett. **63**, 2108 (1989).
[13]J. Shao, W. Lu, X. Lü, F. Yue, Z. Li, S. Guo, and J. Chu, Rev. Sci. Instrum. **77**, 063104 (2006).
[14]X. Lu, D. Beaton, R. Lewis, T. Tiedje, and Y. Zhang, Appl. Phys. Lett. **95**, 041903 (2009).
[15]J. Shao, L. Chen, W. Lu, X. Lü, L. Zhu, S. Guo, L. He, and J. Chu, Appl. Phys. Lett. **96**, 121915 (2010).
[16]D. Gammon, B. Shanabrook, and D. Katzer, Phys. Rev. Lett. **67**, 1547 (1991).
[17]A. Zrenner, L. V. Butov, M. Hagn, G. Abstreiter, G. Böhm, and G. Weimann, Phys. Rev. Lett. **72**, 3382 (1994).
[18]K. Leosson, J. Jensen, W. Langbein, and J. Hvam, Phys. Rev. B **61**, 10322 (2000).
[19]B. Deveaud, A. Regreny, J. Emery, and A. Chomette, J. Appl. Phys. **59**, 1633 (1986).
[20]L. Zhu, J. Shao, X. Lü, S. Guo, and J. Chu, J. Appl. Phys. **109**, 013509 (2011).

[21]J. Shao, D. Haase, A. Dörnen, V. Härle, and F. Scholz, J. Appl. Phys. **87**, 4303 (2000).
[22]J. Shao, R. Winterhoff, A. Dörnen, E. Baars, and J. Chu, Phys. Rev. B **68**, 165327 (2003).
[23]B. Sun, D. Jiang, X. Luo, Z. Xu, Z. Pan, L. Li, and R. Wu, Appl. Phys. Lett. **76**, 2862 (2000).
[24]Q. Zhao, S. Wang, Y. Wei, M. Sadeghi, A. Larsson, and M. Willander, Appl. Phys. Lett. **86**, 121910 (2005).
[25]J. Shao, W. Lu, G. Tsen, S. Guo, and J. Dell, J. Appl. Phys. **112**, 063512 (2012).
[26]S. Imhof, A. Thranhardt, A. Chernikov, M. Koch, N. Koster, K. Kolata, S. Chatterjee, S. Koch, X. Lu, S. Johnson *et al*., Appl. Phys. Lett. **96**, 131115 (2010).
[27]J. Shao, A. Dörnen, R. Winterhoff, and F. Scholz, Phys. Rev. B **66**, 035109 (2002).
[28]H. Xie, J. Katz, W. Wang, and Y. Chang, J. Appl. Phys. **71**, 2844 (1992).
[29]C. Snyder, B. Orr, D. Kessler, and L. Sander, Phys. Rev. Lett. **66**, 3032 (1991).
[30]Y. Song, S. Wang, I. Saha Roy, P. Shi, A. Hallen, and Z. Lai, "Molecular beam epitaxy growth of $InSb_{1-x}Bi_x$ thin films," J. Cryst. Growth (in press).
[31]G. Pettinari, A. Polimeni, J. Blokland, R. Trotta, P. Christianen, M. Capizzi, J. Maan, X. Lu, E. Young, and T. Tiedje, Phys. Rev. B **81**, 235211 (2010).
[32]J. Fan and Y. Chen, J. Appl. Phys. **80**, 1239 (1996).
[33]C. Van de Wall, Phys. Rev. B **39**, 1871 (1989).
[34]J. Lee, J. Kim, and M. Razeghi, Appl. Phys. Lett. **70**, 3266 (1997).